Journal of Alloys and Compounds 323–324 (2001) 279–282

Journal of
ALLOYS
AND COMPOUNDS

www.elsevier.com/locate/jallcom

Preparation and optical properties of nanocrystalline and nanoporous Tb doped alumina and zinc aluminate

M. Zawadzki*, J. Wrzyszcz, W. Strek, D. Hreniak

Institute of Low Temperature and Structure Research, Polish Academy of Sciences, PO Box 1410, 50-950 Wroclaw 2, Poland

---

Abstract

Preparation and morphology of nanocrystalline and nanoporous ceramics composed of a network of alumina and zinc aluminate doped with Tb ions are reported. The pore size distributions are determined by nitrogen adsorption at 77 K. The emission spectra and lifetimes of Tb^{3+} ions were measured. The effect of thermal conditions of preparation on emission properties was investigated. It is concluded that with increasing thermal heating the sizes of nanoparticles increase leading to the cluster formation of Tb^{3+} ions. © 2001 Elsevier Science B.V. All rights reserved.

Keywords: Nanostructures; Chemical synthesis; Optical properties; Luminescence

---

1. Introduction

Nanocrystalline materials characterized by particle diameters less than 100 nm have been the subject of much investigation during the last few years. Such materials demonstrate interesting enhanced optical properties, which may find potential applications as efficient phosphors. The nature of such behaviour has been discussed by many authors in respect of dielectric and semiconducting materials in terms of quantum, confinement effect [1,2]. The effect of confinement on optical behaviour of lanthanide ions in porous γ-Al_2O_3 was reported by Kaplyanski et al. [3,4]. Recently we have reported the optical properties of Eu(III) in nanostructured γ-alumina [5] and zinc aluminate spinels [6] prepared under hydrothermal conditions using basic aluminum salts as Al precursor [7]. We have shown that the emission lifetimes of Eu(III) in these materials exhibited the size effect, i.e. increased with size of nanoparticles.

In this paper we report the preparation of a new class of nanocrystalline and porous ceramics based on alumina and zinc aluminate spinels doped with Tb ions. Their morphology and optical properties were studied. These materials demonstrate interesting emission behavior due to the network of submicron pores and nanosize effects.

2. Experimental results

2.1. Synthesis

Nanocrystalline and nanoporous alumina and zinc aluminate matrixes with high specific surface area and narrow pore size distribution were prepared under hydrothermal conditions. The primary material for the synthesis was aluminum hydroxide produced by hydrolysis of aluminum isoproxide in hot water. The water solution of aluminium hydroxide or aqueous mixture of aluminium hydroxide and zinc acetate (with molar ratio of Al:Zn of 2:1) was hydrothermally treated in an autoclave under pressure below 1 MPa with continuous stirring for some hours. As the result, the sol of aluminum hydroxide or zinc aluminate was obtained, respectively. Both sols were condensed by evaporation (to ~30 wt.%) and then air-dried. Further calcination was performed in a flow of air under temperature steps of 2°/min up to 873 K. The obtained γ-alumina and $ZnAl_2O_4$ materials were used as matrixes for terbium ions. The matrixes were impregnated by an incipient wetness technique using aqueous solution of terbium chlorides to obtain the desired amount of metal in matrix. Such systems were dried and slowly heated again up to 1873 K.

2.2. Characterization

XRD-analysis confirmed that samples prepared through hydrothermal process were single-phase materials — γ-

---

*Corresponding author. Fax: +48-71-441-029.

E-mail address: zawadzki@int.pan.wroc.pl (M. Zawadzki).

PII: S0925-8388(01)01031-3

alumina or $ZnAl_2O_4$ spinel with high crystallite dispersion. Calculated from the broadening of the diffraction peaks using Schererr's formula, mean particle size was 6 and 8 nm, respectively, for γ-alumina and zinc aluminate calcined at 873 K. The nanocrystallinity of the material was retained after thermal treatment at higher temperatures, but an increase in the crystallite size was already noticeable. After heating at 1673 K the matrixes became sintered ceramics with particle size above 50 nm. Moreover, phase change from γ- and θ- to α-alumina was observed.

The presence of terbium in the impregnated matrixes of γ-Al_2O_3 and $ZnAl_2O_4$ was noted by EDAX analysis.

The size and shape of the prepared and calcined matrix particles were investigated by TEM. In the case of both hydrothermally prepared matrixes the morphology is quite uniform — they consist of approximate spherically shaped particles of an average size consistent with those obtained from the XRD patterns. It was found that mean particle size shifts progressively to higher values with increasing calcination temperature, but this increase is much more visible in the case of zinc aluminate matrix. Reported in Fig. 1 is an example of the morphology of $ZnAl_2O_4$ matrix heated at 873 K.

Terbium particles were easily observed in samples with higher Tb loading and heated at higher temperatures; otherwise, terbium was in a very dispersed state. TEM images from the Tb doped alumina and zinc aluminate spinel heated at 1873 K are shown in Figs. 2 and 3, respectively. Terbium oxide particles with well-developed faces of ~50–60 nm in size as well as Al_2O_3 and $ZnAl_2O_4$ matrixes are seen.

The textural properties of alumina and zinc aluminate matrixes obtained from adsorption–desorption isotherms of nitrogen at 77 K by a standard volumetric procedure using the Sorptomatic 1900 FISONS apparatus are collected in Table 1 and related to the temperature of their heat treatment. Both matrixes heated at temperatures below 1273 K give isotherms of type IV with closed hysteresis loops described as type H1 or H2 which suggest the presence of mesopores in the materials. These types of hysteresis loops are characteristic for solids consisting of particles crossed by nearly cylindrical channels or made by aggregates or agglomerates of spheroidal particles. Moreover, such hysteresis loops suggest that pores can have uniform size and shape. The pore size distribution as determined from nitrogen isotherm measurements by application of the Dollimore/Heal method, showed pore radius r_p between 1 and 3 nm for matrix heated at 873 K and 1.2–5.2 or 2–11 nm for alumina and zinc aluminate matrix, respectively, heated at 1323 K with mean pore size r_p depending on heating temperature. These narrow size ranges suggest that hydrothermally obtained matrixes are formed from monodisperse particles. The matrix prepared from Al_2O_3 material exhibits the higher specific surface area which may be correlated with the smaller crystallite size. Alumina matrix is also more resistant to sintering effects occurring after heating at higher temperatures. Thermal treatment of matrixes at 1873 K leads to creation of macroporous materials.

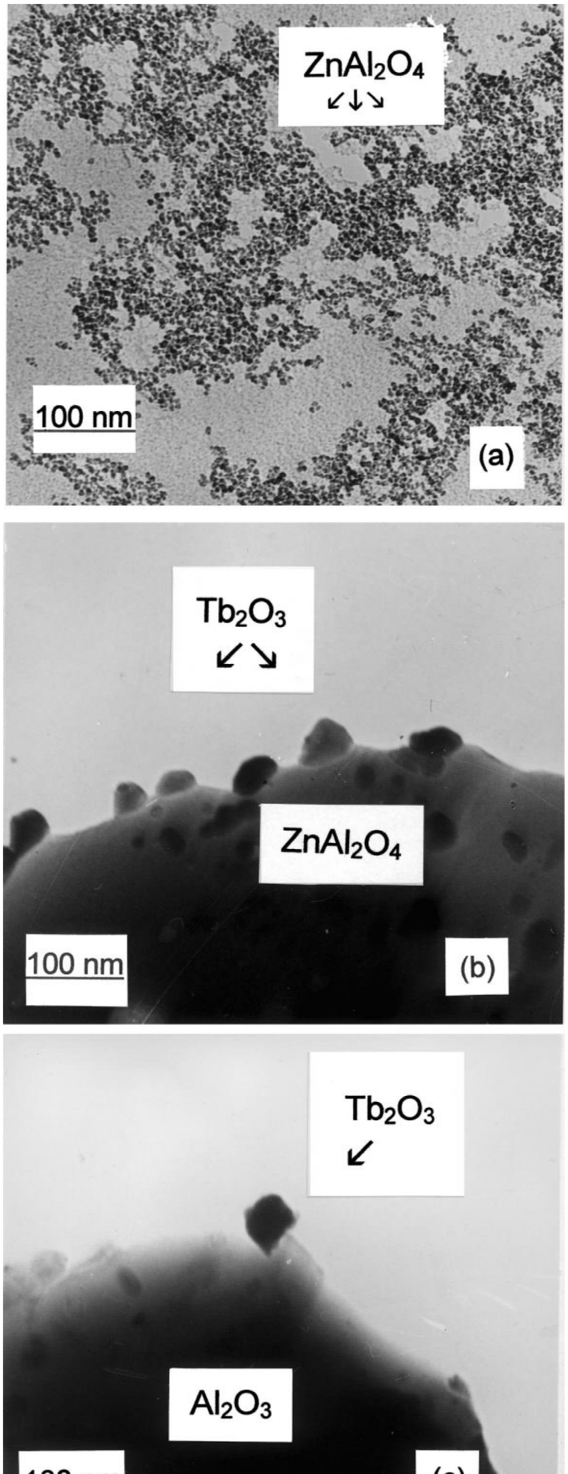

Fig. 1. TEM images of: (a) hydrothermally prepared zinc aluminate matrix heated at 873 K, (b) Tb^{3+} doped zinc aluminate spinel heated at 1873 K, (c) Tb^{3+} doped alumina heated at 1873 K.

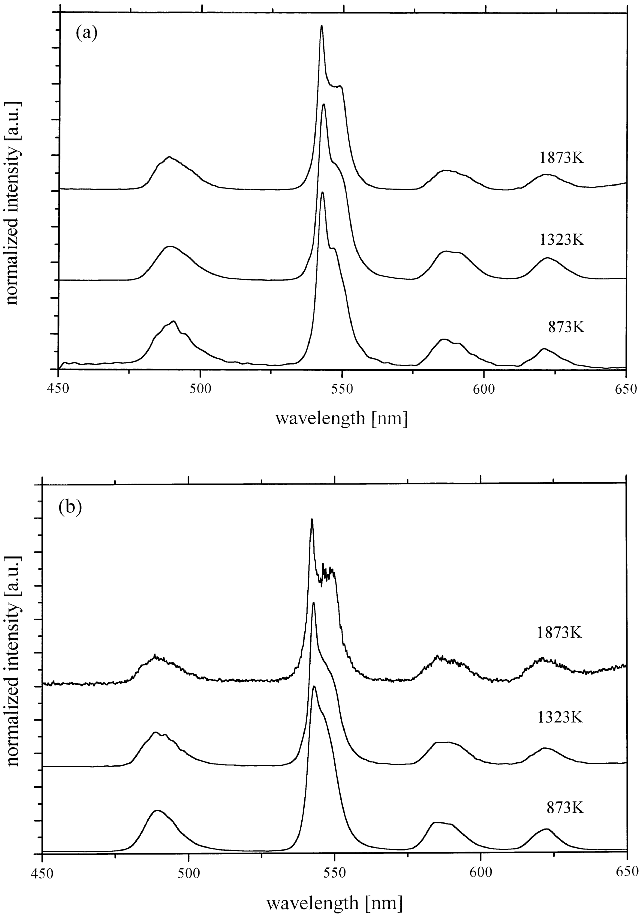

Fig. 2. Emission spectra of Tb^{3+} doped zinc aluminate (a) and alumina (b) nanoparticles in dependence of heating temperature.

3. Optical data and discussion

The emission spectra of Tb doped alumina and zinc aluminate spinel ceramics excited with the 308-nm line of excimer laser are illustrated in Fig. 2.

The emission spectra were normalized to the highest emission peak associated with the green emission of Tb^{3+} arising from the dominant $^5D_4 \rightarrow {}^7F_5$ transition with the peak maximum at 542 nm. The bands associated with the $^5D_4 \rightarrow {}^7F_{6,4,3}$ transitions at 490, 585 and 622 nm were less intense. The observed bands were slightly resolved at lower heating temperature and practically did not change with increasing thermal heating. One can note that the emission spectra of Tb^{3+} in alumina and zinc aluminate spinel particles were very similar.

More information can be obtained from the lifetime measurements because they demonstrated a strong dependence on thermal heating temperature. The emission lifetimes are listed in Table 2. They were perfectly exponential (Fig. 3). One can note that with increasing heating temperature the emission lifetimes decrease significantly.

The emission decay rate is determined by a sum of two radiative k_{rad} and non-radiative k_{nrad} rate constants $k=1/\tau=k_{rad}+k_{nrad}$. The radiative rate should not vary with the size of nanoparticle because it is combined with single ion transition. The non-radiative factor is associated with

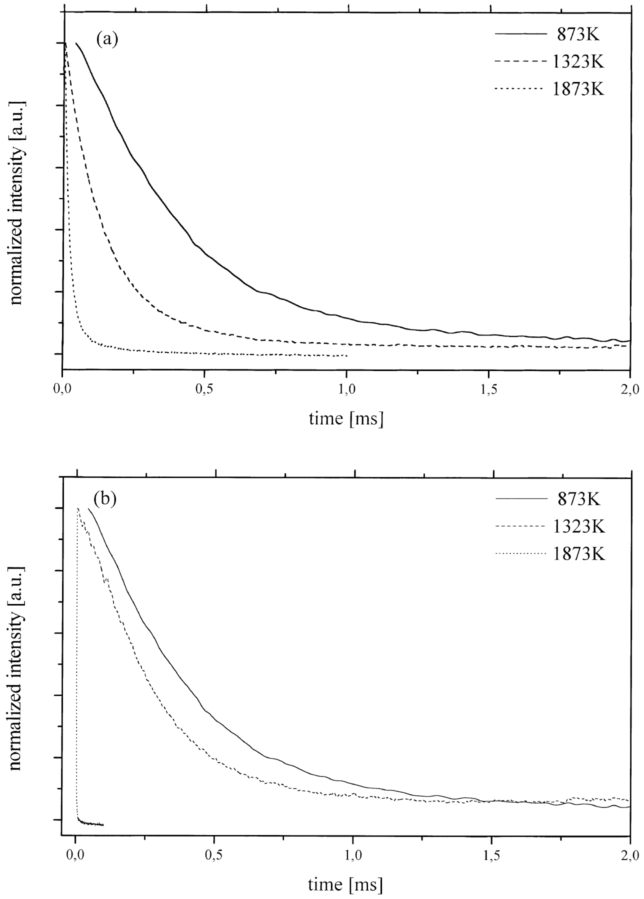

Fig. 3. Emission decay profiles of Tb^{3+} in zinc aluminate (a) and alumina (b) nanoparticles.

Table 1
Specific surface area (S_{BET}), pore size (r_p) and volume (V_p) of the Al_2O_3 and $ZnAl_2O_4$ matrixes heated at different temperatures

Matrix	Heating temperature (K)	S_{BET} (m^2/g)	V_p (cm^3/g)	r_p (nm)
Alumina	873	278	0.38	2.3
	1273	69	0.16	3.8
	1873	Macroporous material		
Zinc aluminate	873	94	0.15	2.2
	1273	12	0.01	9.0
	1873	Macroporous material		

Table 2
Luminescence lifetime $\lambda_{em}=542$ nm ($\lambda_{exc}=308$ nm)

Sample	τ (μs) $T=873$ K	τ (μs) $T=1323$ K	τ (μs) $T=1873$ K
$ZnAl_2O_4$+1% Tb_2O_3	830	190	150
$ZnAl_2O_4$+2% Tb_2O_3	490	150	30
Al_2O_3+2% Tb_2O_3	1350	260	–

multiphonon transitions and energy transfer. One can presume that with increasing thermal heating the multiphonon transitions should decrease because of the diminishing number of high energy OH vibrations. However we observe a quite opposite behaviour in that with increasing thermal heating the emission lifetimes decrease. This means that there exists a competing process leading to shortening observed emission lifetimes. The lifetime observed for Tb^{3+} doped alumina heated at 873 K was the longest, just ~1.3 ms which means that the contribution of non-radiative multiphonon relaxation is negligible. The emission lifetimes measured for the particles heated to higher temperatures decreased their lifetimes five or 18 times for $ZnAl_2O_4$ doped with 1 and 2% Tb_2O_3, respectively. The shortening of emission lifetimes must be associated with formation of aggregates of Tb_2O_3 molecules. The aggregation should also increase with concentration of Tb^{3+} ions which is in fact manifested in lifetime measurements. It is interesting to see that the aggregation is probably much smaller for alumina particles sintered at 873 K because their lifetime is close to a purely radiative one.

We know from the results of Bhargava [8–10] that the emission efficiency increases with decreasing size of nanoparticles. Moreover it was found that the hypersensitive transition intensity increases much more than other f–f transitions. In fact the last effect was not observed in our case. The averaged sizes of alumina and zinc aluminate particles were 4 and 6 nm, respectively, at 873 K. With increasing thermal heating the size of nanoparticles increased up to 50 nm. This may mean that the shortening of lifetimes with increasing temperature cannot be associated with increasing diameters of nanoparticles. We suppose that an increase of nanoparticle size is accompanied by increase of Tb_2O_3 clusters, which are formed in closed pores of alumina and zinc aluminate nanoparticles. This suggests that shortening of emission lifetimes is associated with enhancement of the diffusion of excitation energy of the $^5D_4$ state within the Tb_2O_3 clusters.

Further spectroscopic investigations of the emission nature of terbium ions in nanosize systems are in progress.

4. Conclusions

The proposed method of synthesis of alumina and zinc aluminate spinel seems to be very useful for obtaining nanosize and nanoporous ceramics. Their textural properties make them interesting as a host lattice for active systems such as rare earth ions. It was found that the emission properties of Tb^{3+} were determined by the formation of Tb_2O_3 clusters. This process strongly increases with the temperature of thermal heating of the powders.

Acknowledgements

This research was performed with financial support from the Polish Committee for Scientific Research under Grant no. 3 T09B 063 16.

References

[1] L. Brus, J. Phys. Chem. 90 (1986) 2555.
[2] Y. Wang, N. Herron, J. Phys. Chem. 95 (1991) 525, see references.
[3] A.A. Kaplyanskii, A.N. Kulinkin, A.B. Kutsenko, S.P. Feofilov, T.I. Zakharchenya, T.N. Vasilevskaya, Phys. Solid State 40 (1998) 1310.
[4] J.K. Krebs, S.P. Feofilov, A.A. Kaplyanskii, R.I. Zakharchenya, U. Happek, J. Lumin. 83–84 (1999) 209.
[5] W. Strek, P. Deren, E. Lukowiak, B. Nissen, J. Wrzyszcz, M. Zawadzki, P. Pershukievich, Spectrochim. Acta A 54 (1998) 2121.
[6] W. Strek, P. Deren, A. Bednarkiewicz, M. Zawadzki, J. Wrzyszcz, J. Alloys Comp. 300–301 (2000) 456.
[7] M. Zawadzki, J. Wrzyszcz, Mater. Res. Bull. 35 (2000) 109.
[8] R.N. Bhargava, D. Gallagher, X. Hong, A. Nurmikko, Phys. Rev. Lett. 72 (1994) 416.
[9] R.N. Bhargava, J. Lumin. 70 (1996) 85.
[10] R.N. Bhargava, J. Lumin. 72–74 (1997) 46.